

NORMALIZED STEP SIZE APPROACH TO SIGNAL PROCESSING BASED ON LAGGED CROSS-CORRELATION OF PROBABILITY

¹NAMYONG KIM, ²ANNA ANDONOVA, ³MINGOO KANG

¹Division of electronic, inform. & comm. eng., Kangwon national university, Samcheok, S. Korea

²Faculty of electronic eng. and technologies, Technical university-Sofia, Sofia, Bulgaria

³Division of information and telecommunication engineering, Hanshin university, Osan, S. Korea

E-mail: ¹namyong@kangwon.ac.kr, ²ava@ecad.tu-sofia.bg, ³kangmg@hs.ac.kr

ABSTRACT

The signal processing algorithms based on the lagged cross-correlation of probability (LCCP) have been considered very effective in the multipath environment with impulsive and DC noise coexisting in visual light/power line communication (VLC/PLC) systems for energy saving intelligent buildings. To meet the demand for higher data rates and more complicated sensor node configuration, in this paper, performance enhancement methods by employing a normalized step size in the LCCP-based algorithms which are sensitive to the scaling of system input contaminated with impulses and DC noise are proposed through the analysis of the behavior of optimum weight and the role of magnitude controlled input (MCI) on influence of large errors. The normalized LCCP algorithm with the step size normalized with the averaged power of the current MCI shows a faster speed by about 5 times and has a lower minimum mean squared error by about 3 dB than the conventional LCCP algorithm in blind equalization simulation for indoor VLC/PLC channel models.

Keywords: LCCP, Normalization, Step-Size, DC Bias, Impulsive Noise, VLC/PLC

1. INTRODUCTION

In energy saving buildings white LEDs for illumination are very useful due to their long lifetimes and energy efficiencies. But LEDs are not 100 % efficient at converting input power to light. Some of the energy is converted into heat. For the purpose of further energy efficiency, effective assessment methods of the amount of heat generated by the LED have been studied [1]. When intelligent monitor and control systems through sensor networks are employed in those buildings, about 20% further savings can be yielded in energy usage [2]. Since running wires in buildings cover 50 to 90% of the cost of the sensor networks, wireless communication links are highly recommendable for eliminating that cost [3]. It has been found that sensor node information in smart buildings can be transmitted through the light of those white LEDs modulated at high rates imperceptible to humans both for ambient lighting and for transmitting sensor data [4]. This technology of visible light communication (VLC) for both lighting and communication is considered essential for energy saving buildings as well as implementation with minimal incremental cost [4].

The line-of-sight (LOS) links in indoor VLC systems has small path loss but are susceptible to blockage [5]. On the other hand, the non line-of-sight (NLOS) links utilize reflected paths of the light from indoor surfaces of wall, ceiling and furniture, so that they have strong robustness against blocking, but suffer from multipath problems [6][7]. Other obstacles besides the multipath effect are DC bias noise and impulsive noise. Background solar radiation from windows and ambient lighting are seriously affecting the received sensor signal as DC bias noise. When the illuminations are turned on or off by switches of a room or the sunlight suddenly comes in through the window by unfolding blinds, these ambient lights are playing as a role of DC bias noise in causing decreased sensitivity so that it is required to eliminate the DC noise included in the received signal [8][9]. The DC bias problem may also be mitigated if orthogonal frequency division multiplexing (OFDM) is employed and the OFDM receiver sets the DC carrier to zero as appeared in the work [10]. When the DC noise

changes with time, however, specified adaptive filtering techniques are needed to cope with the problem.

Recently, based on the ubiquitous power line infrastructure and smart grids, integrated systems of VLC and power line communication (PLC) are emerging for sensor networks for energy saving buildings [11][12]. In the integrated VLC/PLC systems where received data from the LED lighting are retransmitted through the sockets of PLC systems, impulsive noise can occur by electrical switch, thermostat operations, plugging and unplugging of electrical plugs, motor starts of electrical devices, power surging on the PLC networks and so on [13]. Therefore, in the integrated VLC/PLC systems DC bias and impulsive noise can occur simultaneously.

For the purpose of dealing with the DC and impulsive noise problems as appeared in VLC/PLC systems as well as multipath problems, adaptive signal processing algorithms based on lagged cross correlation of probability (LCCP) has been developed [14]. The decision feedback (DF) version of LCCP (DF-LCCP) has proved its excellence of performance in the indoor VLC/PLC systems [15]. A recursive approach to the gradient estimation of DF-LCCP for reduced computational complexity has eliminated the constraints of sample size where a large sample size is required for accurate estimation of probability density function (PDF) [16].

In this paper, the behavior of optimum weight of LCCP being robust to large errors due to impulsive noise is investigated and a normalized step size for the LCCP algorithm is proposed for improved performance of LCCP algorithm which is considered a recommendable signal processing algorithm for energy efficient buildings with sensor networks.

This paper is organized as follows. In Section 2, we briefly describe the LCCP function and related algorithms. The magnitude-controlled input (MCI) of LCCP is derived and its role is explained in Section 3. In Section 4, normalized step size with averaged power of MCI is proposed. Section 5 reports simulation results and discussions. Finally, concluding remarks are presented in Section 6.

2. LCCP FUNCTION AND RELATED ALGORITHMS

Defining the probability distribution function (PDF) of transmitted symbols as $f_s(s)$ and the output PDF as $f_y(y)$, the LCCP function $R_{SY}(\tau)$ for two PDFs $f_s(s)$ and the output PDF $f_y(y)$ has been defined in [14] as

$$R_{SY}(\tau) = \int f_s(\alpha) \cdot f_y(\alpha + \tau) d\alpha \quad (1)$$

Under the assumption that the M symbol points $\{S_1, S_2, \dots, S_M\}$ are equiprobable at the transmitter, the $f_s(s)$ can be expressed with Dirac-delta functions $\delta(s)$ as

$$f_s(s) = \frac{1}{M} [\delta(s - S_1) + \delta(s - S_2) + \dots + \delta(s - S_m) + \dots + \delta(s - S_M)] \quad (2)$$

The output PDF $f_y(y)$ for (3) is constructed by the kernel density estimation method as with $G_\sigma(y)$ and a block of N output samples $\{y_k, y_{k-1}, \dots, y_{k-N+1}\}$ (sample size N) [17].

$$f_y(y) \cong \frac{1}{N} \sum_{i=k-N+1}^k G_\sigma(y - y_i) \quad (3)$$

Inserting (2) and (3) into (1) yields

$$R_{SY}(\tau) = \frac{1}{MN} \sum_{i=k-N+1}^k \sum_{m=1}^M G_\sigma(S_m + \tau - y_i) \quad (4)$$

In blind equalization with the linear filter $y_k = \mathbf{W}^T \mathbf{X}_k$ with the weight $\mathbf{W} = [w_0, w_1, w_2, \dots, w_L]^T$ and the input $\mathbf{X}_k = [x_k, x_{k-1}, \dots, x_{k-L+1}, c]^T$ (c is a constant), the lag τ is controllable by w_L and c as

$$\tau = -w_L \cdot c \quad (5)$$

Now for the maximization of $R_{DY}(\tau)$ we can use the steepest ascent method as

$$\mathbf{W}_{new} = \mathbf{W}_{old} + \mu \frac{\partial R_{SY}(\tau)}{\partial \mathbf{W}} \quad (6)$$

By differentiating (5) by the weight, we have the gradient

$$\frac{\partial R_{SY}(\tau)}{\partial \mathbf{W}} = \frac{1}{\sigma^2 NM} \sum_{m=1}^M \sum_{i=k-N+1}^k (S_m - y_i) G_\sigma(S_m - y_i) \mathbf{X}_i \quad (7)$$

Then the LCCP blind algorithm with a step size μ becomes

$$\mathbf{W}_{k+1} = \mathbf{W}_k + \frac{\mu}{\sigma^2 NM} \sum_{m=1}^M \sum_{i=k-N+1}^k (S_m - y_i) G_\sigma(S_m - y_i) \mathbf{X}_i \quad (8)$$

The DF structured DF-LCCP is composed of feed-forward section and feedback section. Then the weight vector of the feed-forward section can be updated by (9). Let the feedback section with Q weights have the weight vector $\mathbf{W}_k^B = [w_{k,0}^B, w_{k,1}^B, w_{k,2}^B, \dots, w_{k,Q-1}^B]^T$ and the decided vector $\hat{\mathbf{D}}_{k-1} = [d_{k-1}^\wedge, d_{k-2}^\wedge, \dots, d_{k-Q}^\wedge]^T$ with d_k^\wedge being the decided symbol for the system output $[\mathbf{W}_k]^T \mathbf{X}_k + [\mathbf{W}_k^B]^T \hat{\mathbf{D}}_{k-1}$. Then the weight update equation for \mathbf{W}_k^B as derived in [14] becomes

$$\mathbf{W}_{k+1}^B = \mathbf{W}_k^B + \frac{\mu}{\sigma^2 NM} \sum_{m=1}^M \sum_{i=k-N+1}^k (S_m - y_i) G_\sigma(S_m - y_i) \hat{\mathbf{D}}_{k+1} \quad (9)$$

The recursive DF-LCCP for reduced computational complexity can be found in [16].

3. MAGNITUDE CONTROLLED INPUT

The term $(S_m - y_i)$ may be defined as an error sample $e_{m,i}$ since the term $(S_m - y_i)$ implies how far the output sample y_i is located from each desired symbol point S_m . Then the gradient (7) can be written as

$$\frac{\partial R_{SY}(\tau)}{\partial \mathbf{W}} = \frac{1}{\sigma^2 NM} \sum_{m=1}^M \sum_{i=k-N+1}^k e_{m,i} G_\sigma(e_{m,i}) \mathbf{X}_i \quad (10)$$

If we consider the sample-averaged operation $\frac{1}{N} \sum_{i=k-N+1}^k (\cdot)$ in (10) can be replaced with the statistical average $E[\cdot]$ or vice versa for practical reasons, we may rewrite (10) as

$$\frac{\partial R_{SY}(\tau)}{\partial \mathbf{W}} = \frac{1}{\sigma^2 M} E[\sum_{m=1}^M e_{m,k} G_\sigma(e_{m,k}) \mathbf{X}_k] \quad (11)$$

At the optimum state of the system with \mathbf{W}^{opt} where $\frac{\partial R_{SY}(\tau)}{\partial \mathbf{W}} = 0$, we have

$$E[\sum_{m=1}^M e_{m,k} G_\sigma(e_{m,k}) \mathbf{X}_k] = 0 \quad (12)$$

On the other hand, the optimum condition of MSE criterion can be expressed as follows [18].

$$E[e_k \mathbf{X}_k] = 0 \quad (13)$$

From the similarity between (12) and (13), we may notice that e_k of MSE criterion may correspond to $e_{m,k}$ of the LCCP criterion and \mathbf{X}_k of MSE criterion can correspond to $G_\sigma(e_{m,k}) \mathbf{X}_k$ as a modified input vector. This input modification implies that the magnitude of \mathbf{X}_k is controlled by $G_\sigma(e_{m,k})$. If $e_{m,k}$ is negligibly small, the magnitude of \mathbf{X}_k is unchanged, but when $e_{m,k}$ is a large value, the magnitude of \mathbf{X}_k is reduced. Knowing that large error samples $e_{m,k}$ can make the algorithm (9) unstable, we can expect that the input modification may play an essential role in robustness of the LCCP algorithm against impulsive noise under which $e_{m,k}$ can become a very large value. In this regard, it is appropriate that the term $G_\sigma(e_{m,k}) \mathbf{X}_k$ in (12) can be interpreted as a magnitude-controlled version of \mathbf{X}_k , so that we



may define $\mathbf{X}_{m,k}^{MCI}$ as a magnitude controlled input (MCI) in (14).

$$\mathbf{X}_{m,k}^{MCI} = G_{\sigma}(e_{m,k})\mathbf{X}_k \quad (14)$$

Besides that the MCI in (14) keeps the algorithm stable even at the occurrences of large error by impulse noise, we may wonder if the averaging process $\frac{1}{NM} \sum_{m=1}^M \sum_{i=k-N+1}^k$ in (9) or (11) could mitigate the influence of impulses. But it does not seem to contribute much to blocking the influence of large errors since even an impulse can dominate the averaging operation.

4. POWER ESTIMATION OF MCI FOR NORMALIZED STEP SIZE

Similar to the NLMS (normalized LMS) that employs the modified step size that is normalized by the averaged power of the current input samples as introduced in [18][19], we propose two types of normalized step sizes μ_{NLCCP1} and μ_{NLCCP2} for justification of the role of MCI $\mathbf{X}_{m,k}^{MCI}$ in robustness against impulsive noise as

$$\mu_{NLCCP1} = \frac{\mu}{\frac{1}{M} \sum_{m=1}^M |x_{k-m}|^2} \quad (15)$$

$$\mu_{NLCCP2} = \frac{\mu}{\frac{1}{M} \sum_{m=1}^M |x_{m,k}^{MCI}|^2} \quad (16)$$

where $x_{m,k}^{MCI} = G_{\sigma}(e_{m,k})x_k$ is from (14).

Considering the fact that impulses can defeat the average operation as explained in Section 3, we may notice that the denominator of (15) or (16) may become large in an incident with impulsive noise. That means that impulsive noise can make those step sizes very small, so that it may induce a very slow convergence. To avoid this kind of situations, we need to track the averaged power $P_{ave}(k)$ and $Q_{ave}(k)$ recursively as

$$P_{ave}(k) = \beta \cdot P_{ave}(k-1) + (1-\beta) \cdot \frac{1}{M} \sum_{m=1}^M |x_{k-m}|^2 \quad (17)$$

$$Q_{ave}(k) = \beta \cdot Q_{ave}(k-1) + (1-\beta) \cdot \frac{1}{M} \sum_{m=1}^M |x_{m,k}^{MCI}|^2 \quad (18)$$

where β ($0 < \beta < 1$) .

The equations (17) and (18) can be expressed in the following z-transformed transfer function

$A(z)$ with its input $\frac{1}{M} \sum_{m=1}^M |x_{k-m}|^2$ and output $P_{ave}(k)$, $\frac{1}{M} \sum_{m=1}^M |x_{m,k}^{MCI}|^2$ and output $Q_{ave}(k)$, respectively.

$$A(z) = (1-\beta) \frac{z}{z-\beta} \quad (19)$$

The parameter β controls the time constant of the single-pole low-pass filter $A(z)$. Then the resulting LCCP-based algorithms become

$$\mathbf{W}_{k+1} = \mathbf{W}_k + \frac{\mu}{P_{ave}(k)\sigma^2 NM} \sum_{m=1}^M \sum_{i=k-N+1}^k e_{m,i} \mathbf{X}_{m,i}^{MCI} \quad (20)$$

$$\mathbf{W}_{k+1} = \mathbf{W}_k + \frac{\mu}{Q_{ave}(k)\sigma^2 NM} \sum_{m=1}^M \sum_{i=k-N+1}^k e_{m,i} \mathbf{X}_{m,i}^{MCI} \quad (21)$$

For convenience's sake, equation (20) and (21) will be referred to in this paper as the normalized LCCP1 (NLCCP1) and NLCCP2, respectively. Their DF versions, DF-NLCCP1 and DF-NLCCP2 are easily derived only by replacing the step size μ of the DF-LCCP in (9) and the work [13]

with $\frac{\mu}{P_{ave}(k)}$ and $\frac{\mu}{Q_{ave}(k)}$.

5. RESULTS AND DISCUSSION

In this section the effectiveness of the proposed NLCCP1 and NLCCP2 will be investigated in the VLC/PLC environments with their DF versions. As in [7] for VLC, bi-polar symbol $\{+1,-1\}$ ($M=2$) is transmitted through the channel of NLOS links in indoor VLC systems. The impulse response of NLOS links in VLC systems vary from room to room. The impulse responses for this simulation are worked out by the authors in [7] where they took an empty typical office room with a transmitter and two field-of-view (FOV) receivers $Rx1$ (40°) and

Rx2 (132°). They found that 132° FOV is more prone to be affected by ISI, so that we opt the FOV 132° for this simulation. They also found that ISI has large influence on data rate performance at higher rates above 100 Mb/s. So we opt to use the following normalized impulse responses $H_1(z)$ for 150 Mb/s and $H_2(z)$ for 200 Mb/s data rate as used in [7] and [15].

$$H_1(z) = 0.1478 + 0.7540z^{-1} + 0.5737z^{-2} + 0.2455z^{-3} + 0.1217z^{-4} + 0.0674z^{-5} + 0.0282z^{-6} + 0.0087z^{-7} \quad (22)$$

$$H_2(z) = 0.3041 + 0.6595z^{-1} + 0.5512z^{-2} + 0.3497z^{-3} + 0.1711z^{-4} + 0.1064z^{-5} + 0.0608z^{-6} + 0.0418z^{-7} + 0.0190z^{-8} + 0.0076z^{-9} \quad (23)$$

The impulsive noise n_k composed of additive Gaussian white noise (AWGN) and impulses is generated according to the following PDF of Gaussian mixture model [15][20].

$$f_N(n_k) = \frac{1-\varepsilon}{\sigma_{GN}\sqrt{2\pi}} \exp\left[-\frac{n_k^2}{2\sigma_{GN}^2}\right] + \frac{\varepsilon}{\sqrt{2\pi(\sigma_{GN}^2 + \sigma_{IN}^2)}} \exp\left[-\frac{n_k^2}{2(\sigma_{GN}^2 + \sigma_{IN}^2)}\right] \quad (24)$$

where incident rate of the impulse ε , the variance of AWGN σ_{GN}^2 , and impulse variance σ_{IN}^2 are 0.0012, 0.001, and 50, respectively. Also the varying DC bias noise $1 \cdot \sin(2\pi k / 40000)$ starts to be added to the received signal from sample time $k = 20000$ as depicted in Figure 1.

The feed forward filter length of the DF filter is 11 and its backward filter length is 4. The kernel size is $\sigma = 0.6$ and the sample size is $N = 2$. The convergence parameter $\mu = 0.008$ is used for comparison at more complete convergence unlike 0.01 used in [15].

MSE performance for varying DC bias and impulsive noise is shown in Figure 2 for $H_1(z)$ and in Figure 4 for $H_2(z)$. The well-known constant modulus algorithm with DF (DF-CMA) in [18][20] fails to converge even before the varying DC bias is added. When the DC bias begins

to increase after the sample time $k=20000$, DF-correntropy in [20] that has completely converged starts to show increasing MSE according to the DC bias increasing.

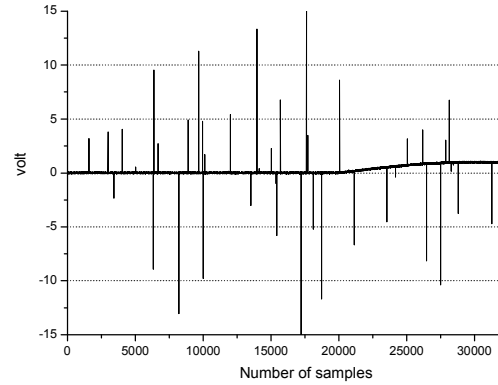


Figure 1: An Example of Noise composed of AWGN, Impulsive and DC Bias for Simulation

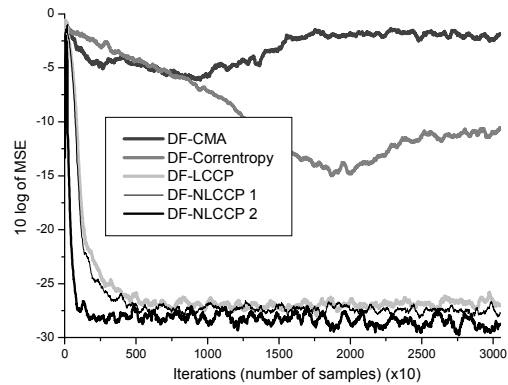


Figure 2: MSE Learning Performance under $H_1(z)$ with Impulsive Noise and Varying DC Bias.

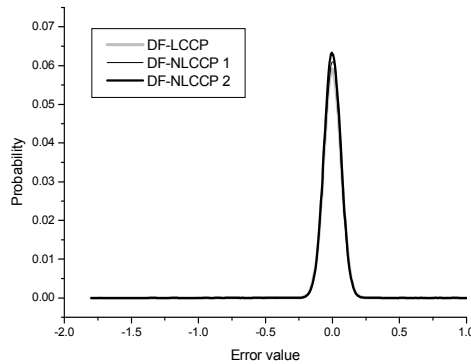


Figure 3: Error Distribution for $H_1(z)$ with Impulsive Noise and Varying DC Bias.

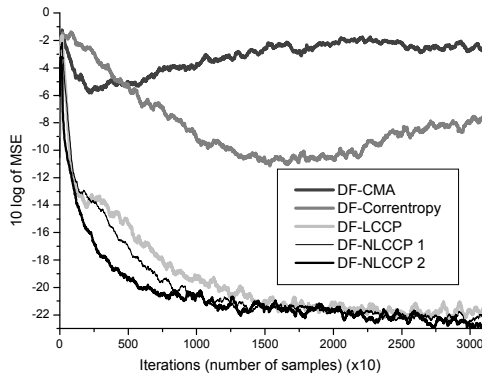


Figure 4: MSE Learning Performance under $H_2(z)$ with Impulsive Noise and Varying DC Bias.

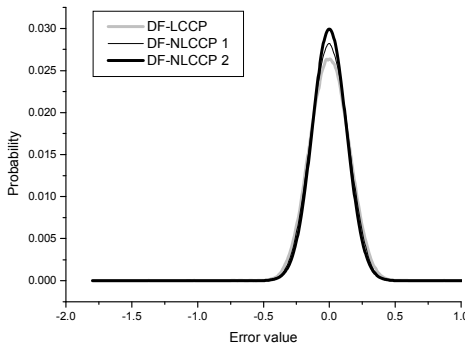


Figure 5: Error Distribution for $H_2(z)$ with Impulsive Noise and Varying DC Bias.

But the DF-LCCP type algorithms converge rapidly for both channel models being left undisturbed by the increasing DC bias noise. In the case of the 150 Mb/s channel $H_1(z)$, the DF-LCCP and DF-NLCCP1 show similar learning performance converging in about 5000 samples, but DF-NLCCP1 has a lower steady state MSE by about 1 dB. On the other hand, the DF-NLCCP2 converges in about 1000 samples showing the lowest steady state MSE decreased by about 3 dB when compared to DF-LCCP. The similar performance enhancement is observed in the 200 Mb/s channel $H_2(z)$ in Figure 4 as well.

From the comparison of DF-LCCP and DF-NLCCP1 where DF-NLCCP1 shows faster convergence speed, the difference of steady state MSE is about 1 dB. The steady state MSE of DF-NLCCP2 is lower than that of DF-LCCP by about 2 dB.

The superior performance of the proposed DF-NLCCP2 against varying DC and impulsive noise

can be observed also in the comparison of error distribution depicted in Figure 3 and 5 for $H_1(z)$ and $H_2(z)$, respectively. All the DF-LCCP type algorithms form a very concentrated distribution only on zero implying successful compensation for the DC noise for both channels. The error samples gather around zero with slight differences of concentration. The peak probability at zero for $H_1(z)$ is 0.059 for DF-LCCP, 0.061 for DF-NLCCP1, and 0.063 for DF-NLCCP2, respectively. Similarly, the peak probability for $H_2(z)$ is 0.026, 0.028, and 0.03 for DF-LCCP, DF-NLCCP1, and DF-NLCCP2, respectively. These results indicate that the DF-NLCCP2 has the highest peak probability among all those algorithms being compared.

6. CONCLUSION

The DF-LCCP algorithm is known to outperform MSE-based DF-CMA and other correntropy-based algorithms in the multipath environment where impulsive and DC noise are coexisting. This property is considered very useful in wireless VLC/PLC systems for sensor networks of energy saving intelligent buildings. Though the problem of computational complexity of the DF-LCCP algorithm has been solved for practical reasons by recursive gradient estimation method in previous related works, its learning speed and error performance are needed to be more enhanced due to ever increasing number of sensor nodes and data rate. One of the methods for performance enhancement is to employ a time varying step size that controls the LCCP-based algorithms sensitive to the scaling of its input contaminated with impulses. In this paper, through the analysis of the behavior of optimum weight and the role of MCI on mitigation of influence from large error, NLCCP algorithm has been proposed that employs the step size normalized with the averaged power of the current MCI elements. For justification of the role of MCI in robustness against impulsive noise, two types of normalized step sizes are introduced and experimented with DF versions of LCCP through simulation.

The normalized step size using input itself without magnitude control shows a small enhancement of performance as in convergence speed, minimum MSE, and error distribution. On the other hand, the one using MCI shows a faster speed by about 5 times and a lower minimum MSE by about 3 dB in channel model $H_1(z)$ and 2 dB in $H_2(z)$, compared to DF-LCCP algorithm. These



results lead us to conclude that the step size normalization with the MIC power is significantly effective in the VLC/PLC systems for energy saving smart buildings.

ACKNOWLEDGEMENT

This study was supported by 2014 Research Grant from Kangwon National University (No. 220140076)

REFERENCES:

- [1] A. Andonova, N. Kim, and N. Vakrilov, "Estimation the amount of heat generated by LEDs under different operating conditions", *Elektronika ir Elektrotechnika*, Vol. 22, No. 2, March 2016, pp. 49-53.
- [2] Q. Huang, X. Li, M. Shaurette, and R. Cox, "A novel sensor network architecture for intelligent building environment monitoring and management", *Proceedings of the 2011 ASCE international workshop on computing in civil engineering*, Miami, FL., June 2011, pp. 347-354.
- [3] C. Lin, C. Federspiel, and D. Auslander, "Multi-sensor single-actuator control of HVAC systems", <http://www.cbe.berkeley.edu/research/briefs-wirelessxyz.htm>.
- [4] S. Zhao and J. Xu and O. Trescases, "Burst-mode resonant LLC converter for an LED luminaire with integrated visible light communication for smart buildings", *IEEE Transactions on Power Electronics*, Vol. 29, Aug. 2014, pp. 4392 – 4402.
- [5] K. Cui, G. Chen, Z. Xu, and R. Roberts, "Line-of-sight visible light communication system design and demonstration", *Proceedings of CSNDSP 2010*, Newcastle, Tyne, July, 2010, pp. 621-625.
- [6] J. Carruthers, S. Carroll, and P. Kannan, "Propagation modelling for indoor optical wireless communications using fast multi-receiver channel estimation", *Optoelectronics, IEE Proceedings*, Vol.150, Oct. 2003, pp. 473–481.
- [7] Z. Dong, K. Cui, G. Chen, and Z. Xu, "Non-line-of-sight link performance study for indoor visible light communication systems", *Proceedings of SPIE Photonics and Optics – Free Space Laser Communications IX*, San Diego, CA, Aug. 2010, pp. 781404-1 - 781404-10.
- [8] J. Choi, "Performance analysis of the VLC system with Z-HBT line coding", *Proceedings of ISCIT 2009*, Icheon, Korea, Sep. 2009, pp. 1242-1246.
- [9] M. Saadi and L. Wattisuttikulkij, "Visible light communication: opportunities, challenges and channel models", <http://www.cennser.org/IJJEI/eiV02N01/ei020101.pdf>.
- [10] J. Armstrong, "OFDM for optical communications", *Journal of Light Wave Technology*, Vol. 27, Feb. 2009, pp. 189-204.
- [11] H. Lee, Y. Kim, and K. Sohn, "Optical wireless sensor networks based on VLC with PLC-Ethernet interface", *World Academy of Science, Engineering and Technology*, Vol. 57, July, 2011, pp. 245-248.
- [12] S. Alavi, A. Supaat, S. Idrus, and S. Yusof, "Integrated system of visible free space optic with PLC", *Proceedings of MICC 2009*, Kuala Lumpur, Malaysia, Dec. 2009, pp. 271-275.
- [13] H. Chaouche, F. Gauthier, A. Zeddani, M. Tlich, and M. Machmoum, "Time domain modeling of powerline impulsive noise at its source", *Journal of Electromagnetic Analysis and Applications*, Vol. 3, Sept. 2011, pp. 359-367.
- [14] N. Kim, K. Kwon and Y. You, "Lagged cross-correlation of probability density functions and application to blind equalization", *JCN*, Vol. 14, Oct. 2012, pp. 540-545.
- [15] N. Kim and H. Byun, "Indoor sensor data transmission for energy-saving buildings", *Proceedings of ESPCO 2013*, Venice, Italy, Sep. 2013, pp. 71-75.
- [16] N. Kim, "Decision Feedback Equalization for Indoor Visual Light Communication", *International Journal of Circuits Systems and Signal Processing*, Vol. 8, Aug. 2014, pp.47-53.
- [17] E. Parzen, "On the estimation of a probability density function and the mode", *Ann. Math. Stat.* Vol. 33, 1962, p. 1065.
- [18] S. Haykin, *Adaptive Filter Theory*, Prentice Hall, Upper Saddle River, 4th edition, 2001.
- [19] R. Chinaboina, D. Ramkiran, H. Khan, M. Usha, B. Madhav, K. Srinivas & G. Ganesh, "Adaptive algorithms for acoustic echo cancellation in speech processing", *IJRRAS*, Vol. 7, April 2011, pp. 38-42.
- [20] I. Santamaria, P. Pokharel, and J. Principe, "Generalized correlation function: definition, properties, and application to blind equalization", *IEEE Trans. Signal Processing*, Vol. 54, June 2006, pp. 2187-2197.